Structural and dynamical properties of YH_3

P. van Gelderen,[1,2] P. J. Kelly,[1] and G. Brocks[1]
[1]*Faculty of Applied Physics and MESA+ Research Institute, University of Twente, P.O. Box 217, 7500 AE Enschede, The Netherlands*
[2]*Electronic Structure of Materials and Research Institute for Materials, Faculty of Sciences, University of Nijmegen Toernooiveld 1, 6525 ED Nijmegen, The Netherlands*
(Received 15 July 2002; published 12 September 2003)

On the basis of parameter-free electronic structure calculations for YH_3, it was predicted that the total energy of the high symmetry HoD_3 structure deduced from neutron powder diffraction (NPD) experiments on YD_3 could be lowered by small displacements of the hydrogen atoms. Subsequent, more detailed NPD experiments failed to observe any such symmetry-breaking displacements, but neither could they be ruled out. Moreover, a new broken symmetry structure which is slightly different to that predicted by total energy calculations was proposed. Analysis of the phonon modes measured very recently using Raman spectroscopy yields the first clearcut experimental evidence for symmetry breaking. Here we present the results of parameter-free lattice dynamics calculations for each of three structures currently being considered for YH_3. The results are obtained within the harmonic model starting from a force field which is calculated from first principles in a supercell geometry. Comparison of the calculated phonon densities of states with the experimental spectrum determined by inelastic neutron scattering gives clear evidence for a broken symmetry structure. The Debije-Waller factors for some of the hydrogen atoms are exceptionally large and we speculate on the importance of the large zero-point motions of these atoms for the structure of YH_3.

DOI: 10.1103/PhysRevB.68.094302 PACS number(s): 63.20.Dj, 71.30.+h, 61.66.−f, 71.15.Pd

I. INTRODUCTION

Interest in metal-hydrogen systems was rekindled by the discovery of reversible effects which occur when hydrogen is absorbed and desorbed.[1–3] Huiberts *et al.*[1] found that, when exposed to hydrogen gas, thin films of yttrium and lanthanum exhibit a metal-insulator transition as a function of the hydrogen content. The β-YH_2 phase is formed when sufficient hydrogen has been absorbed to form a dihydride. The resistivity of this phase is about a factor 5 lower than that of pure metallic yttrium and YH_2 is a good reflector for visible wavelengths. Further increase of the hydrogen content leads to nucleation of the γ-YH_3 phase. At a hydrogen-to-yttrium ratio of about 2.8 the resistivity increases sharply and the film becomes transparent to visible light. From the position of the absorption edge in substoichiometric $YH_{3-\delta}$ with $\delta \sim 0.1$, an optical gap close to 2.7 eV was deduced[4,5] for YH_3. The large increase in resistivity when the trihydride phase is formed, as well as its negative temperature coefficient and inverse proportionality to δ in $YH_{3-\delta}$ suggest that YH_3 is a true semiconductor. However, so far the size of the fundamental gap has not been determined experimentally. If the H_2 pressure is reduced sufficiently, hydrogen desorbs until the dihydride phase is recovered. Since the process of switching between the reflecting dihydride and the transparent trihydride phase is reversible, these ''switchable mirrors'' may become suitable for a number of different applications.

At the time of their discovery a good understanding of the mechanism underlying the metal-insulator transition in these materials was lacking. The properties of YH_2 had been studied by Weaver *et al.*[6,7] and successfully interpreted on the basis of self-consistent electronic structure calculations by Peterman *et al.*[8] However, straightforward application of band theory to YH_3 failed to produce a gap. Using band structure calculations based upon the local density approximation (LDA) to density functional theory (DFT), Dekker *et al.*[9] and Wang and Chou[10] considered a number of possible lattice structures for YH_3 but did not succeed in finding a structure with a band gap. At the time, the only evidence that YH_3 had the structure first determined for HoD_3 by Mannsmann and Wallace[11] was a rather brief early report of a neutron diffraction structure determination for YD_3 by Miron *et al.*[12] This quite complicated HoD_3 structure has 24 atoms in a hexagonal unit cell which is tripled in the basal *ab* plane. The HoD_3 structure of YD_3 was recently confirmed by Udovic *et al.*[13] in neutron powder diffraction (NPD) experiments and even more recently by Remhof *et al.*[14] for epitaxially grown films of the type used in the switching experiments.[15] For the HoD_3 structure, both theoretical studies found a band structure characteristic of a semimetal with a large band overlap of about 1.3 eV (Ref. 10) at the center of the Brillouin zone.

The failure of DFT-LDA calculations to explain the large band gap in YH_3 and LaH_3 prompted theoretical work into the nature of the band gap in these materials. Kelly *et al.* argued that the zero-value band gap found by LDA for LaH_3, for instance, made the problem similar to Ge, which also has a vanishing gap in LDA. In fact it is well known that DFT-LDA severely underestimates band gaps.[16,17] Approximations based upon an improved treatment of the long-range electron-electron interaction—more specifically the *GW* approximation[18,19]—reproduce experimental band gaps of semiconductors and insulators very well.[19–21] Our recent *GW* calculations predict a fundamental gap of 1 eV for YH_3 in the HoD_3 structure.[22] The optical gap is much larger (3 eV) due to vanishing matrix elements for optical transitions at lower energies. These results are in general agreement with experiments on the yttrium hydrides and a more detailed discussion can be found in Ref. 23.

In this paper we focus on the structure and lattice dynam-

ics of YH_3. Although DFT-LDA is not very suitable for calculating excitation spectra, it does give accurate ground state properties, such as the charge density and the equilibrium structure. Kelly *et al.* found from such a calculation that small displacements of hydrogen atoms in YH_3 which break the symmetry of the HoD_3 structure, lower the total energy and open up a gap in the LDA band structure.[24] A *GW* calculation of the quasiparticle spectrum also produces a large gap for YH_3 in the broken symmetry structure. Its band structure looks quite similar to that of YH_3 in the HoD_3 structure, so from optical experiments it will be quite difficult to distinguish between the two structures.[4]

In the NPD experiments by Udovic *et al.* on YD_3,[13] which were refined using the HoD_3 structure, unusually large anisotropic temperature factors are found for the deuterium atoms, in particular for the so-called ''metal-plane'' deuterium atoms located in or close to the planes containing the yttrium atoms. Udovic *et al.* proposed a measure of disorder on the ''metal-plane'' deuterium sublattice and incorporated this in their refinement by defining additional, fractionally occupied sites for these atoms. The atoms involved in this ''fractional disorder'' are exactly those atoms which are displaced from their high symmetry positions in the proposed broken symmetry structure. The small additional Bragg peaks which should be associated with the proposed symmetry-lowering however were not found in low temperature NPD experiments.[25] It is conceivable though that large hydrogen zero point motion could reconcile the measured powder diffraction pattern with the broken symmetry structure.[26] Solid state nuclear magnetic resonance (NMR) experiments[27] which probe the local symmetry of the deuterium sites, could not be interpreted using the HoD_3 structure, which would indicate a symmetry breaking. In addition, in a more recent paper on neutron diffraction experiments on thin epitaxial YD_3 films it was suggested that the diffraction data are not only consistent with the $P\bar{3}c1$ space group of the HoD_3 structure, but also with the less symmetric $P6_3cm$ space group.[28] These results have reopened the discussion on the lattice structure of YH_3.[29]

Recently Kierey *et al.*[30] performed Raman spectroscopy experiments on YH_3; from a symmetry analysis of the Raman-active phonon modes they concluded that their YH_3 films must have either $P6_3cm$ or $P6_3$ symmetry. The latter is the space group of the ''broken symmetry structure'' with the lowest total energy from the LDA calculations. LDA calculations on YH_3 with a lattice structure constrained to have $P6_3cm$ symmetry result in a total energy which is between those of the HoD_3 and the $P6_3$ broken symmetry structures; its band structure is almost identical to that of the HoD_3 structure.

In the present work we reconsider the prediction of the LDA total energy calculations that YH_3 has the structure with $P6_3$ symmetry, and give a full account of a recent short report of a parameter-free lattice dynamics study on YH_3.[31] We present the calculated phonon dispersion curves of YD_3 and YH_3 in the HoD_3 structure ($P\bar{3}c1$ symmetry), in the broken-symmetry structure ($P6_3$ symmetry) and in the recently proposed lattice structure with $P6_3cm$ symmetry. We calculate the root mean square displacements of the atoms in each of the Cartesian directions, the Debije-Waller factors, as well as the ellipsoids of thermal and zero point motion using the eigenvalues and eigenvectors of the dynamical matrix. The Debije-Waller factors can be compared directly to the values derived from the NPD experiments for YD_3. They may reveal whether the additional peaks expected for a broken symmetry structure have escaped detection as a result of large zero point motions. We also compare the calculated eigenvalues of the dynamical matrix directly to the energies and symmetries of the observed optical modes in the Raman experiments. In addition we interpret the neutron vibrational spectroscopy (NVS) data for YH_3 obtained by Udovic *et al.* using inelastic neutron scattering.[29,32] From the calculated eigenvectors we can identify the modes of vibration which predominate in particular energy ranges. We will show that the experimental results are better explained by a broken symmetry structure rather than the HoD_3 structure.

In Sec. II the computational methods for calculating the lattice vibrations are briefly discussed, Secs. III and IV contain the main results on YH_3 and YD_3, respectively, and in Sec. V the main conclusions are discussed. The Appendix contains a short discussion of the lattice vibrations of Si, and serves as a check on our computational method.

II. CALCULATION OF LATTICE VIBRATIONS

A thorough discussion of lattice dynamics in the harmonic approximation can be found in textbooks (see, e.g., Madelung[33]) and monographs (see, e.g., Brüesch[34]). Here we present a short account of the theory, mainly to clarify the notation. The crystal potential energy is expanded up to second order in the displacements $u_{n\alpha i}$ of the atoms from their equilibrium positions, where n labels the unit cells, α the atoms in the unit cell, and i the three Cartesian directions

$$U = U_0 + \frac{1}{2} \sum_{\substack{n\alpha i \\ n'\alpha' i'}} \Phi_{n\alpha i}^{n'\alpha' i'} u_{n\alpha i} u_{n'\alpha' i'}, \qquad (1)$$

where U_0 is the energy of the equilibrium structure. The force constants $\Phi_{n\alpha i}^{n'\alpha' i'}$ can be obtained from the reaction force on atom α in the nth cell in the ith direction when atom α' in cell n' is displaced in direction i'. Making use of the lattice periodicity, the solutions of the lattice dynamical problem can be labeled by a wave vector $\mathbf{q}$. They are the eigenmodes of the dynamical matrix

$$D_{\alpha i}^{\alpha' i'}(\mathbf{q}) = \frac{1}{\sqrt{m_\alpha m_{\alpha'}}} \sum_n \Phi_{n\alpha i}^{0\alpha' i'} e^{i\mathbf{q}\cdot(\mathbf{R}_{0\alpha'} - \mathbf{R}_{n\alpha})}, \qquad (2)$$

where m_α is the atomic mass of atom α and $\mathbf{R}_{n\alpha}$ gives the equilibrium position of atom α in unit cell n in real space; unit cell 0 is chosen as the reference unit cell. In principle the summation in Eq. (2) extends to unit cells at infinity, but in practice it can be truncated since the reaction forces become negligibly small at large distances.

It is possible to determine the force constants $\Phi_{n\alpha i}^{0\alpha' i'}$ from DFT-LDA calculations without introducing any arbitrary fit-

ting parameters. There are basically two ways of doing this. The linear response method approaches the problem by calculating the inverse of the dielectric matrix[35,36] and has been successfully applied to a number of semiconductors,[37,38] and metals.[39] It can be used to calculate the dynamical matrix for general **q** vectors.

In the so-called direct method, the force constants are calculated using a supercell geometry. In the method used here, we displace a specific atom in a specific direction and calculate the forces on all the other atoms in the supercell from the self-consistent charge density of the disturbed system via the Hellmann-Feynman theorem (see, e.g., Ref. 40). This calculation is repeated for each symmetry independent atom and direction. The direct method was used for simple metals,[41,42] for semiconductors,[43] and for insulators.[44,45] Calculated phonon frequencies are usually very accurate and agree with the experimental data within a few percent. In semiconductors and insulators with nonvanishing Born effective charges the longitudinal optical (LO) modes at $\mathbf{q}=0$ are not obtained correctly within a finite supercell since the incomplete electrostatic screening in such systems leads to long-range interatomic force constants.[45] The long-range interactions can be included in the dynamical matrix if the Born effective charge tensors and the dielectric constant ϵ_∞ are known.[45–47] These quantities can be obtained using linear response theory.[38,48,49] From the interplanar force constants obtained in supercell calculations Kunc and Martin[50] have used an alternative way to calculate the correct frequencies for the LO vibrations. Kern *et al.*[51] have recently described its application in detail; we will use their approach.

The eigenvalues of the dynamical matrix of Eq. (2) are the squared eigenfrequencies $\omega_j^2(\mathbf{q})$ of the oscillators. The band index j labels the $3r$ phonon branches of a solid with r atoms in the unit cell. From the phonon band structure $\omega_j(\mathbf{q})$, it is straightforward to find the corresponding density of states. The eigenvectors $Q_{j\alpha i}(\mathbf{q})$ describe the contribution from the jth phonon mode with wave vector $\mathbf{q}$ to the displacement of atom α in the direction i; they describe which atoms are moving in which direction for each mode. We can calculate partial densities of states which tell us how particular atoms move in particular directions as a function of phonon energy, which is very useful for the interpretation of inelastic neutron scattering experiments. The partial phonon density of states for displacement of atom α in direction i is given by

$$G_{\alpha i}(\omega)=\frac{V}{(2\pi)^3}\sum_j \int_{\mathrm{BZ}}|Q_{j\alpha i}(\mathbf{q})|^2\delta[\omega-\omega_j(\mathbf{q})]d\mathbf{q}, \tag{3}$$

where V is the unit cell volume. The total phonon density of states is then obtained by a summation over α and i.

For a solid at a temperature T the mean number of phonons with energy $\hbar\omega_j(\mathbf{q})$ is given by the Bose-Einstein distribution $n_{j\mathbf{q}}(T)=\{\exp[\hbar\omega_j(\mathbf{q})/k_BT]-1\}^{-1}$. The mean square displacement of a single quantum mechanical harmonic oscillator, $\langle u^2\rangle=(\hbar/m\omega)(n+\frac{1}{2})$, is easily generalized to that of a single atom α in the direction i as

$$\langle u_{\alpha i}^2\rangle=\frac{V}{(2\pi)^3}\frac{\hbar}{m_\alpha}\sum_j \int_{\mathrm{BZ}}|Q_{j\alpha i}(\mathbf{q})|^2\frac{[n_{j\mathbf{q}}(T)+\frac{1}{2}]}{\omega_j(\mathbf{q})}d\mathbf{q}. \tag{4}$$

It is evident from this expression that light atoms, such as hydrogen, vibrating at low frequencies exhibit large zero point motions. To calculate Eq. (4) we use Eq. (3) to transform the sum over modes j and $\mathbf{q}$ vectors into an integral which includes the partial density of states $G_{\alpha i}(\omega)$. The off-diagonal elements $\langle u_{\alpha i}u_{\alpha j}\rangle$ can be calculated in an analogous fashion.

The thermal and zero point motion of the atoms is often described using the matrix of anisotropic temperature factors **B** (see, e.g., Willis and Pryor[52]). For atom α it is defined by

$$B_{ij}(\alpha)=8\pi^2\langle u_{\alpha i}u_{\alpha j}\rangle. \tag{5}$$

Diagonalizing this symmetric matrix yields the lengths and directions of the main axes of the ellipsoid of thermal or zero point motion. Evidently, the form of **B** is restricted by the symmetry of the atomic site in the crystal. For example, the full cubic symmetry in silicon restricts the ellipsoids of vibration of the atoms to spheres. Moreover, equivalent atoms, the positions of which are related by a symmetry operation, have ellipsoids related by symmetry. These symmetries of **B** provide a way to check the internal consistency of the calculations.

The relative intensity of a diffraction peak corresponding to reciprocal lattice vector **K** in a powder diffraction pattern can be obtained from

$$I(\mathbf{K})\sim\left|\sum_\alpha \exp(i\mathbf{K}\cdot\mathbf{R}_{0\alpha})f_\alpha(\mathbf{K})\exp[-W_\alpha(\mathbf{K})]\right|^2. \tag{6}$$

The atomic scattering factors for neutron scattering $f_\alpha(\mathbf{K})$ are **K** independent and can be found in standard tables. The Debije-Waller factor $W_\alpha(\mathbf{K})$

$$W_\alpha(\mathbf{K})=\frac{1}{16\pi^2}\sum_{ij} K_iK_jB_{ij}(\alpha) \tag{7}$$

describes the reduction of the scattered intensity at **K** resulting from the thermal vibration of atom α. Consequently, the intensity of the peaks in the diffraction spectra that correspond to large **K** in combination with large B_{ij} are most affected by atomic motions.

III. RESULTS FOR YH_3

In order to estimate the accuracy of the calculated phonon spectra test calculations were made for silicon using the direct supercell method with supercells containing 54 and 250 atoms. The results show good agreement with experiment and are summarized in the Appendix; very reasonable dispersion curves are already obtained using the smaller supercell. In this section we present our results for YH_3 in the HoD_3 and broken symmetry structures. We begin by describing these structures in more detail.

A. The proposed lattice structures for YH_3

The HoD_3 and broken symmetry structures are closely related. They are shown schematically in Fig. 1. One can describe these structures starting from a hexagonal lattice consisting of *ABAB* stacked planes of yttrium atoms. In Fig. 1 the yttrium ''metal'' planes are indicated by solid lines; one is positioned at $z=+c/4$ and the other at $z=-c/4$. The hexagonal lattice contains two interstitial sites per metal atom which have local tetrahedral symmetry. Of every three hydrogen atoms in YH_3 two are found close to the tetrahedral sites; we shall denote these atoms by H(T). The third hydrogen atom, which we shall denote H(M), is located in, or close to, the metal plane. Optimizing this structure with a Y_2H_6 unit cell results in the so-called LaF_3 structure. It has one H(M) atom in each of the two metal planes, while the four H(T) atoms (which are not shown in Fig. 1) move slightly away from their ideal tetrahedral positions and are located in planes at about $z=\pm 0.09c$ and $z=\pm 0.41c$. The equilibrium unit cell is about 15 % larger than the unit cell volume of pure metallic yttrium, almost entirely as a result of an elongation of the c axis.

The HoD_3 and broken symmetry structures can be obtained from the LaF_3 structure by tripling it in the basal *ab* plane such that there are three metal-plane hydrogen atoms in each metal plane. In the HoD_3 structure, two of these three atoms move slightly away from the metal plane. One moves to a position about $0.07c$ above the metal plane, the other to a position about $0.07c$ below the metal plane. The third H(M) stays exactly in the metal plane. This displacement is sketched schematically in Fig. 1(a) in a plane containing the c axis and the H(M) atoms. The lines represent the metal planes and the open circles represent the H(M) atoms. The plane shown is a glide plane with a translation vector of $c/2$ in the z direction; the space group of the HoD_3 structure is $P\bar{3}c1$. As a consequence of the out-of-plane H(M) displacements the H(T) atoms are also slightly displaced, as described in detail in Refs. 10 and 24. The tripled hexagonal unit cell contains 24 atoms with a stoichiometry Y_6H_{18}. The total energy of the HoD_3 structure is lower than that of the LaF_3 structure.[10]

In the broken symmetry structure which corresponds to the lowest total energy in LDA calculations the unit cell is also tripled with respect to the LaF_3 structure.[24] But now *all* the H(M) atoms move out of the metal plane, one third of them by about $0.07c$, one third by about $-0.07c$, and the rest by about $0.03c$ [see Fig. 1(b)]. The displacements are *different* for H(M) atoms which are related by a translation of $c/2$ in the z direction. For example, when a H(M) atom in the lower metal plane moves up by about $+0.07c$, the related atom in the upper metal plane moves up by about $0.03c$ and vice versa. The remaining related pair of H(M) atoms are displaced by the same amount with respect to the metal planes, i.e., by about $-0.07c$. Comparing this structure to the HoD_3 structure we observe that the glide and inversion symmetries of the HoD_3 structure are broken. They are replaced by a screw axis through the H(M) atoms that are displaced by $-0.07c$. The space group for this broken symmetry structure is $P6_3$. Again, the H(T) atoms are also slightly displaced as compared to their positions in the LaF_3 structure.

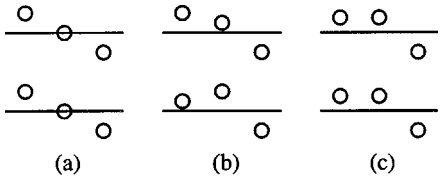

FIG. 1. Schematic outline of the proposed lattice structures for YH_3, with (a) the HoD_3 structure with $P\bar{3}c1$ symmetry, and the broken symmetry structures with (b) $P6_3$ and (c) $P6_3cm$ symmetry, respectively. The horizontal lines indicate the planes formed by the yttrium atoms in the *ab* plane. The c axis is in the plane of the paper and the open circles denote the H(M) hydrogen atoms; the H(T) atoms are not shown.

Recently a new lattice structure with $P6_3cm$ symmetry has been proposed in which all the H(M) atoms are also displaced out of the metal plane. As in the HoD_3 structure, the displacements are identical for H(M) atoms which are related by a translation of $c/2$ in the z direction. Two out of every three H(M) atoms are displaced by about $0.05c$ and the remaining H(M) atoms by about $-0.07c$, see Fig. 1(c). Since all the H(M) atoms are displaced out of the metal plane this structure has no inversion center. Instead, there is both a screw axis through the H(M) atoms that are displaced

TABLE I. Wyckoff positions of the yttrium (Y), tetrahedral hydrogen [H(T)], and the metal-plane hydrogen [H(M)] atoms in the proposed lattice structures of YH_3 in the HoD_3 structure with $P\bar{3}c1$ symmetry, and the broken symmetry structures with $P6_3$ and $P6_3cm$ symmetries. The numbers are obtained upon optimizing these structures in a $(2\times2\times2)$ supercell using Γ-point only sampling of the Brillouin zone.

	$P\bar{3}c1$	$P6_3$	$P6_3cm$
Y	$6f$	$6c$	$6c$
	$x=0.663$	$x=0.667$	$x=0.669$
		$y=-0.003$	
		$z=0.250$	$z=0.250$
$H_1(T)$	$12g$	$6c$	$6c$
	$x=0.348$	$x=0.345$	$x=0.306$
	$y=0.025$	$y=-0.015$	
	$z=0.093$	$z=0.093$	$z=0.091$
$H_2(T)$		$6c$	$6c$
		$x=-0.308$	$x=-0.354$
		$y=-0.042$	
		$z=-0.093$	$z=-0.092$
$H_1(M)$	$4d$	$2a$	$4b$
	$z=0.181$	$z=-0.316$	$z=0.200$
$H_2(M)$	$2a$	$2b$	$2a$
		$z=0.184$	$z=0.324$
$H_3(M)$		$2b$	
		$z=-0.216$	

by $-0.07c$, and a glide plane, which is the plane containing the c axis and the H(M) atoms. In Table I we summarize the details of the three proposed lattice structures for YH_3.

In the following discussion we shall focus especially upon the positions and the zero point motion of the H(M) atoms in the c direction. These atoms play a key role in the symmetry lowering when going from the HoD_3 structure to either of the $P6_3cm$ or $P6_3$ broken symmetry structures. We note that, starting from the HoD_3 structure, a symmetry lowering can be achieved in four different but equivalent ways. For example, the four representations of the $P6_3$ broken symmetry structure can be transformed into each other by applying those symmetry elements of the HoD_3 structure which no longer apply to this broken symmetry structure (glide and inversion). The ''average'' of these four equivalent broken symmetry structures has the high symmetry of the HoD_3 structure.

B. Computational details

We use the direct supercell method for calculating the phonon dispersion curves for YH_3 within the harmonic approximation for the three lattice structures described above. The supercell is defined by doubling the unit cell in each of the three lattice directions; this $(2\times2\times2)$ cell contains 192 atoms. The inequivalent atoms α' in the reference unit cell are displaced one at a time by 0.1 a.u. (0.052918 Å) in each of the three Cartesian directions i' and the self-consistent charge density is recalculated for each perturbed structure. Using this new charge density we determine the Hellmann-Feynman forces on all other atoms $n\alpha$ in the supercell, see Eqs. (1) and (2). The force constant $\Phi_{n\alpha i}^{0\alpha' i'}$ between the displaced atom α' and an arbitrary atom in the supercell is then given by the ratio of the force in a particular direction on the atom $n\alpha i$ in the supercell and the amplitude of the given displacement. In order to remove (small) contributions from third order (and higher odd order) terms in the crystal potential, we use displacements in positive and negative direction and average the force constants. The full space group symmetry of the solid is used to keep the number of calculations to a minimum.

Having generated all the force constants we symmetrize the results by applying the symmetry elements to all atoms and averaging the resulting force fields. For a finite supercell, the force constants resulting from atoms on the boundary of the supercell are small, but not zero. Following Parlinski *et al.*,[44] we include images of atoms that lie on the boundary of the supercell. Each image of these atoms is included in the calculation with a fractional weight which depends upon the geometry of the supercell. We include all the generated force constants in our calculation of the phonon bands, also if shells of atoms are incomplete as a consequence of the shape of the supercell. In this way we almost perfectly obey the translational sum rule, which demands that the sum of all the forces in the supercell vanishes:

$$\sum_{n\alpha} \Phi_{n\alpha i}^{0\alpha' i'} = 0. \tag{8}$$

This sum rule should hold for each direction i, and for each atom α' displaced in each Cartesian direction i'. Small deviations from the sum rule due to nonharmonic contributions or numerical errors result in the frequencies of the acoustic modes not going to zero at $\mathbf{q}=0$. To enforce the sum rule we change for each i and for each α' and i' the force constant $\Phi_{0\alpha' i}^{0\alpha' i'}$ by the difference between the force on the displaced atom and the sum of all forces on the atoms which were not displaced. These corrections are small but ensure that the acoustic modes behave physically near $\mathbf{q}=0$. The other bands show negligible changes.

Once the time-consuming self-consistent supercell calculations have been performed and the force constants have been obtained, the dynamical matrix is constructed for any $\mathbf{q}$ and diagonalized, see Eq. (2). Since this is only a 72×72 matrix for a solid with 24 atoms in the unit cell, this last step is not computationally demanding.

The ground state properties of the supercells described in this work are calculated using a Car-Parrinello type electronic structure code.[53–55] For reasons of efficiency we sample only the Γ point of the Brillouin zone. We comment upon this in the next subsection. The one-electron wave functions within DFT-LDA are expanded in a plane wave basis, including functions up to a kinetic energy cutoff of 30 Rydberg. Soft Troullier-Martins pseudopotentials were used,[56] which were generated as described in Refs. 10 and 57. Nonlinear core corrections[58] are included for yttrium.

C. Supercell and Brillouin zone sampling

The accuracy of the calculated phonon eigenvectors and eigenfrequencies depends on the size of the supercell used to calculate the atomic force constants. Ideally it should be so large that all forces vanish at the boundaries of the cell, but this is never fully achieved in practice. As a result of this, atoms inside the supercell experience forces not only from the displacement of the atom inside their own cell but also from the periodic images of that displaced atom. Atoms outside the supercell on the other hand, are considered not to experience any forces. Both of these effects contribute to systematic errors in the dispersion curves. Phonon frequencies of modes that fit within the supercell geometry do not suffer from this type of error.

A problem related to the use of a finite supercell is the approximation of the Brillouin zone summation in the calculation of the self-consistent charge density and the total energy by a single $\mathbf{k}$ point, in our case the Γ point. Since the Γ-point approximation becomes better as the supercell size is increased, and we need a large supercell to calculate the force constants anyway, we have not attempted to calculate the forces with an improved $\mathbf{k}$-point sampling. We have carried out a number of tests of the BZ summation in order to estimate the reliability of the Γ-point sampling for the $Y_{48}H_{144}$ supercell ($=2\times2\times2\times Y_6H_{18}$) used in most of our calculations.

We compare a number of highly converged total energy differences, calculated with primitive unit cells and dense BZ samplings,[10,24] with those obtained with the $Y_{48}H_{144}$ supercell and Γ-point sampling. As a reference we use a high

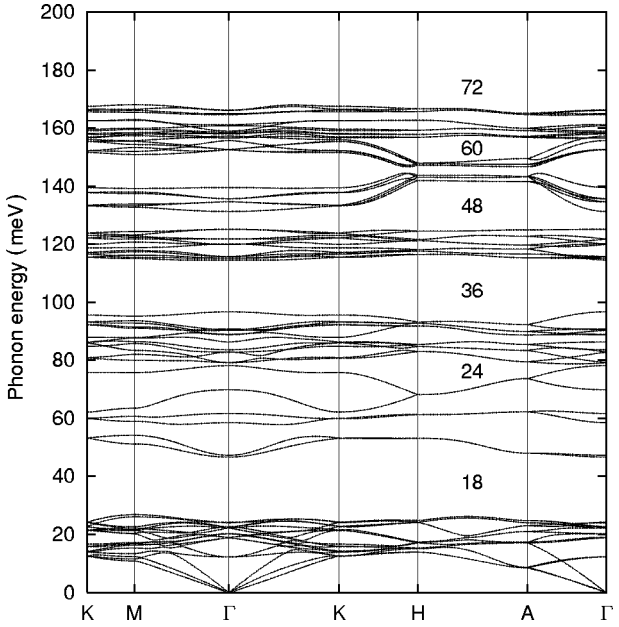

FIG. 2. Calculated phonon dispersion curves for YH_3 in the broken symmetry structure with $P6_3$ symmetry. The numbers between H and A give the total number of bands starting from 0 meV.

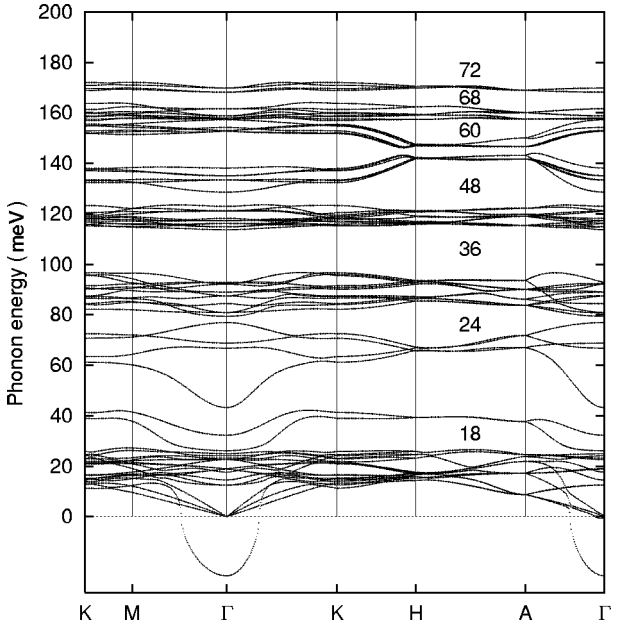

FIG. 3. As the previous figure for YH_3 in the HoD_3 structure. For the soft mode solutions with $\omega^2<0$ we plot the real quantity $i\omega$.

symmetry Y_2H_6 lattice in which the hydrogen atoms are located in the tetrahedral H(T) and octahedral H(O) positions of the hexagonal yttrium lattice. Increasing the nearest-neighbor H(T)-H(T) distance from 0.25c to 0.30c, and moving the H(O) atoms into the metal planes to become H(M) atoms we find from our supercell calculations a decrease in the total energy of 985 meV/YH_3 which is to be compared to the values of 980 meV/YH_3 reported by Wang and Chou,[10] and 965 meV/YH_3 reported by Kelly *et al.*[24] The total energy difference between the HoD_3 structure and the broken symmetry structure with $P6_3$ symmetry is 16 meV/Y_6H_{18}, as compared to 40 meV found by Kelly *et al.*[59] For the Γ-only $Y_{48}H_{144}$ supercell, the total energy of the lattice structure with $P6_3cm$ symmetry lies between the total energies of the HoD_3 structure and of the broken symmetry structure with $P6_3$ symmetry.

We conclude from these tests that the Γ-point sampling is quite good. We can understand this in terms of the very low and vanishing density of states at the Fermi level for the HoD_3 and broken symmetry structures, respectively. For a (near) semiconductor a special-point type of sampling should be quite good and this is achieved using the supercell.

D. Phonon band structures

The calculated phonon band structure for YH_3 in the broken symmetry structure ($P6_3$ symmetry, Fig. 1) is shown in Fig. 2 along some high symmetry directions in the Brillouin zone. With 24 atoms in the unit cell there are in total 72 bands. The lowest 18 branches are dominated by the low frequency motion of yttrium which, with an atomic weight of 89, is essentially decoupled from the hydrogen motion. The hydrogen atoms are well separated from one another by the large yttrium atoms. This and the tripling of the unit cell leads to a large number of almost dispersionless hydrogen-related phonon bands. Unfortunately there are no experimental **q**-resolved spectra with which we can compare, since bulk YH_3 crystals of the type needed for neutron scattering measurements disintegrate into powder because of the large volume change associated with the hydrogen absorption. However, in the next section we will use the vibrational density of states to interpret NVS data, which can be obtained from powder samples.

The nearly complete decoupling of the eigenmodes of the yttrium and hydrogen sublattices and the fact that pure yttrium is also hexagonal allows for a comparison of the calculated low frequency modes with dispersion curves which have been measured for pure yttrium.[60] The energies and dispersions are found to be quite comparable and the differences can to a large degree be attributed to the substantial elongation of the c axis in YH_3.

For YH_3 in the broken symmetry structure which corresponds to an electronic band structure with a gap, we have checked in detail the relevance of long-range force constants by explicitly using the correction method described by Kern *et al.*[51] for the dispersions along ΓA. The planar force constants between a displaced atom in the center and the plane of atoms on the edge of the supercell give an upper bound for the effect of long-range forces. Including such corrections only slightly modifies the frequencies of the LO modes at Γ. It does not change the frequencies of other special **q** points which fit exactly in our supercell geometry. As the dispersions of the optical modes are very small anyway, we have neglected these corrections in further calculations.

We have also calculated the lattice dynamics for YH_3 in the HoD_3 structure ($P\bar{3}c1$ symmetry, Fig. 1); the corresponding phonon band structure is shown in Fig. 3. Since both structures are very similar, so are their phonon bands. However, there is one major difference. For the HoD_3 structure we find a soft mode close to Γ where, because $\omega^2<0$,

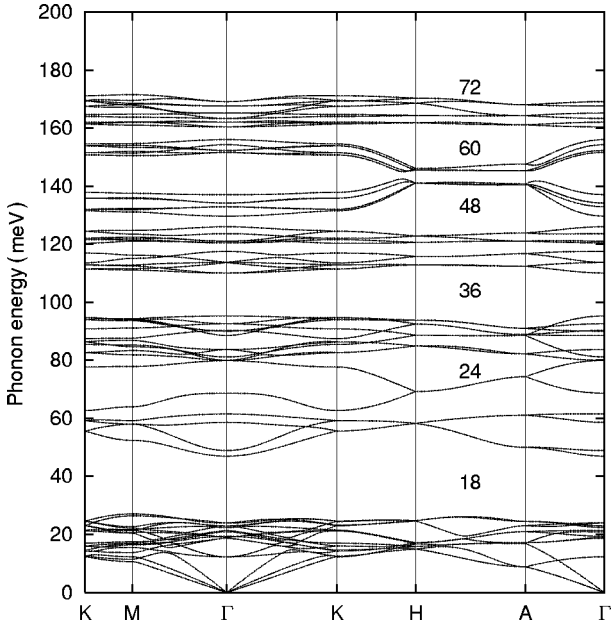

FIG. 4. As the previous figure for YH_3 in the broken symmetry structure with $P6_3cm$ symmetry.

we plot the real quantity $i\omega$. This shows that the HoD_3 structure is unstable, i.e., there are atomic displacements which can lower the energy. The position of the minimum of ω^2 is at $\mathbf{q}=0$. This implies that a lower total energy structure exists in the same unit cell. Inspection of the calculated eigenvector of the soft mode reveals that it moves both H(M) atoms which are exactly in the metal plane in the HoD_3 structure, out of this plane. This is indeed the essential difference between the HoD_3 and broken symmetry ($P6_3$) structures. The soft mode for YH_3 in the HoD_3 structure is a restatement of the earlier finding by explicit energy minimization that the broken symmetry structure has a lower total energy.[24]

For YH_3 in the lattice structure with $P6_3cm$ symmetry, Fig. 1, we obtain the band structure shown in Fig. 4. The phonon band structure is quite similar to that of the $P6_3$ symmetry structure of Fig. 2. There is no soft mode in Fig. 4 although YH_3 in the $P6_3$ structure has a lower total energy. This is because the displacements needed to transform the $P6_3cm$ structure into the $P6_3$ structure do not simply correspond to an eigenmode of YH_3 in the $P6_3cm$ structure. In detail there are important differences between the calculated lattice dynamical properties of the $P6_3cm$ and $P6_3$ structures, which are discussed below.

E. Raman and infrared spectra

The calculated phonon eigenfrequencies and eigenmodes at Γ can be compared to the results of the Raman experiments by Kierey *et al.*[30] From a symmetry analysis of the experimentally observed modes Kierey *et al.* concluded that there is no inversion symmetry in the YH_3 lattice. The HoD_3 structure has $P\bar{3}c1$ symmetry which includes an inversion center. Consequently, on the basis of these Raman experiments the HoD_3 structure was ruled out as a possible lattice structure for YH_3. In Table II we compare our calculated phonon frequencies with the frequencies obtained from the Raman experiments, labeled with their point group symmetry at Γ. We omit the results we have obtained for the HoD_3 structure because these have an incorrect symmetry. Both for the $P6_3cm$ structure and the $P6_3$ structure the calculated and experimental frequencies agree reasonably well; one would perhaps have a slight preference for the $P6_3cm$ structure from these data. It should be borne in mind, however, that this conclusion is based upon the fact that of the many modes of the system only a limited number appear in the experimental Raman spectrum.

TABLE II. Comparison of the experimentally observed Raman frequencies by Kierey (Ref. 30) with the calculated frequencies of the correct symmetry, for the broken symmetry structures with $P6_3$ and $P6_3cm$ symmetry. The energies are in meV.

Symmetry	Exp.	$P6_3$	$P6_3cm$
E_1	19.0	18.8	18.7
A_1	23.3	24.0	22.9
A_1	54.9	58.5	58.6
A_1	60.5	61.7	61.6
A_1	76.9	78.1	80.0
A_1	81.2	83.6	80.7
E_1	90.0	88.8	89.8
E_2	92.2	90.3	92.4
A_1	97.2	96.7	95.0
E_1	112.3	115.7	113.5
E_1	161.2	161.0	162.0

A few vibrational modes were also identified by Lee and Shin[5] in optical experiments on $YH_{3-\delta}$; their corresponding frequencies are 77, 112, and 156 meV. They can be identified from the list of calculated frequencies of both the $P6_3cm$ and $P6_3$ symmetry structures, see Table II, but again the data are insufficient to distinguish between these two structures.

F. Densities of states and NVS experiments

The densities of states (DOS) corresponding to the phonon dispersions shown in Figs. 2–4 are plotted in Fig. 5. The neutron vibrational spectroscopy (NVS) experiments on YH_x (and LaH_x) powders by Udovic *et al.*[29,32] measure the energy loss of inelastically scattered neutrons which is closely related to the phonon total density of states. The experimental high resolution data[29] are plotted in Fig. 5(b) for x nominally equal to 3. From the partial densities of states calculated using Eq. (3), we find that the low energy vibrational modes (below 30 meV) are dominated by yttrium and that hydrogen atoms hardly participate in the motions at these energies. Yttrium vibrations account for the lowest 18 bands in Fig. 2. The vibrations at energies above 40 meV (the remaining 54 bands) involve almost exclusively hydrogen atoms.

In all three structures the frequencies of the hydrogen vibrations are grouped in bands separated by gaps, which results in well-defined peaks in the phonon density of states, see Fig. 5. We observe large differences between the frequencies of modes corresponding to vibrations in the *ab*

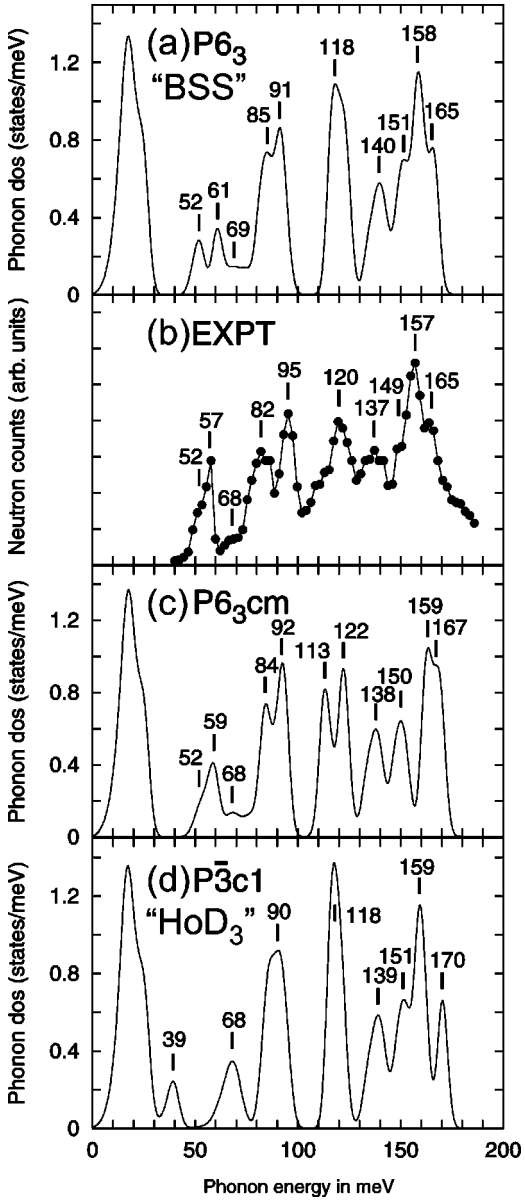

FIG. 5. (a) Calculated total phonon densities of states for YH_3 in the broken symmetry structure with $P6_3$ symmetry. The data have been broadened using a Gaussian line shape of width 12 meV. The numbers indicate the maxima, or peak positions. (b) Experimental neutron vibrational spectroscopy data taken from Ref. 29. (c) Calculated total phonon densities of states for YH_3 in the structure with $P6_3cm$ symmetry and (d) the HoD_3 structure with $P\bar{3}c1$ symmetry, respectively.

plane and those in which the atoms oscillate in the *c* direction. This is illustrated by Fig. 6 where the partial densities of states of the $P6_3$ broken symmetry structure is plotted for the H(T) and H(M) atoms, projected onto displacements in the basal plane and along the *c* axis. The difference is most striking for the H(M) atoms. These can move relatively freely in open channels along the *c* direction but are laterally constrained in the *ab* plane by the metal atoms in that plane. The former motion leads to low frequency modes with energies between 50 and 100 meV, whereas the *ab* plane oscillations of the H(M) atoms give high frequency modes with

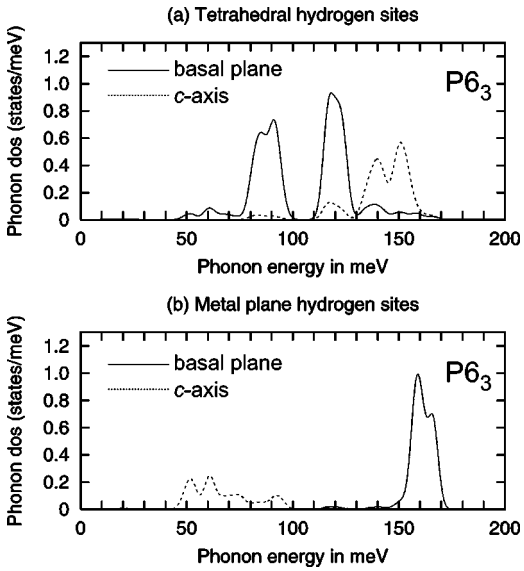

FIG. 6. Partial phonon densities of states for the $P6_3$ symmetry structure calculated by projecting on (a) the H(T) and (b) the H(M) atoms, and oscillations in the basal *ab* plane (solid lines) and in *c*-axis directions (dashed lines), respectively.

energies between 150 and 170 meV. The separation in energy between basal plane and longitudinal vibrations of the H(T) sublattice is smaller. The corresponding *ab* plane oscillations have energies between 80 and 100 meV, and between 110 and 130 meV. The vibrations of the H(T) atoms in the *c* direction have frequencies mainly between 130 and 160 meV. As it turns out, the pattern of splitting of the peaks can be rationalized reasonably well in terms of local vibrations of hydrogen atoms about the symmetry-independent (Wyckoff) positions. The relative intensities of these peaks then correspond to the occupation ratios of the Wyckoff positions. Where appropriate, this simple rationalization will be used to interpret the results.

In Table III we compare the peak positions in the calculated phonon density of states of the three structures to the peak energies obtained from the NVS experiments for YH_3 (exp.). Most calculated peaks have energies that compare reasonably well to the experimental data, but there are essential differences. We will discuss these starting from the low

TABLE III. Positions of calculated peaks in the (broadened) phonon density of states for the three possible structures. The experimental data are obtained from the high-resolution NVS spectrum of Udovic *et al.* (Ref. 29). The energies are in meV.

$P6_3$	$P\bar{3}c1$	$P6_3cm$	Exp.	Vibrations
52	39	52	52	H(M)$\parallel c$
61		59	57	H(M)$\parallel c$
69	68	68	68	H(M)$\parallel c$
85		84	82	H(T)$\perp c$
91	90	92	95	H(T)$\perp c$
118	118	122	120	H(T)$\perp c$
140	139	138	137	H(T)$\parallel c$
158	159	159	157	H(M)$\perp c$

frequency modes which are dominated by H(M) vibrations along the c direction. In the $P6_3$ broken symmetry structure the H(M) atoms are divided over three different Wyckoff positions, see Fig. 1(b), which gives rise to three peaks at slightly different energies. Each of these peaks represents two bands; they include bands 19 to 24, see Fig. 2. In the calculations we find two sharp peaks at 52 and 61 meV and a broad peak at 69 meV. That these peaks indeed correspond to H(M) vibrations along the c direction can be seen in Fig. 6. In the NVS experiment, there is a single strong peak at 57 meV and a shoulder at 52 meV. In the HoD_3 structure with $P\bar{3}c1$ symmetry there are only two Wyckoff positions for the H(M) atoms with an occupation ratio of 2:1. Udovic *et al.* suggested that the two experimental peaks and their relative intensity are evidence for the existence of only two Wyckoff positions consistent with the HoD_3 structure.[29,32] Instead, we suggest that the broad feature in the NVS data near 68 meV corresponds to the broad peak at 69 meV in the calculated density of states of the $P6_3$ broken symmetry structure. In the low energy range 40–70 meV, the calculated density of states of the $P6_3cm$ symmetry structure of Fig. 5 (c) also gives very good agreement with experiment. In the $P6_3cm$ symmetry again only two H(M) Wyckoff positions are present which are occupied in a ratio of 2:1. The singly occupied Wyckoff site corresponds to the atoms which are displaced slightly further from the metal plane. The c-axis motions of these atoms have a frequency of about 68 meV.

The calculated phonon density of states for the HoD_3 structure ($P\bar{3}c1$) is shown in Fig. 5(d) where we have ignored the soft mode and its imaginary frequency. The agreement with experiment is much poorer. The peak corresponding to the motion along the c axis of the H(M) atoms located exactly in the yttrium plane, cf. Fig. 1(a), which corresponds to the bands 19 and 20 in Fig. 3, has an energy of 39 meV, which is too low compared to the experimental feature at 52–57 meV. It even partially overlaps with the highest frequency yttrium vibrations. Part of its intensity is lost to the soft mode at imaginary frequencies. The peak related to the vibrations along the c axis of the out-of-plane H(M) atoms (the 4 bands 21–24 in Fig. 3) is at 68 meV, which is about 10 meV higher than the experimental feature.

The next feature in the experimental spectrum is formed by two relatively strong peaks at 82 and 95 meV. All three lattice structures exhibit strong phonon DOS peaks in this energy range, but their shapes and splittings differ. The peaks corresponding to bands 25–36 in Figs. 2–4 are mainly composed of vibrations of the H(T) atoms in the ab plane, see Fig. 6. In the HoD_3 ($P\bar{3}c1$) structure all 12 bands lead to essentially one peak at 90 meV, Fig. 5(d), whereas in the $P6_3cm$ and $P6_3$ broken symmetry structures we find two peaks at (84, 92) and (85, 91) meV, respectively, each of which corresponds to 6 bands. In the experimental spectrum there is a clear splitting between two peaks at 82 and 95 meV with approximately equal intensity. It will be obvious that this agrees reasonably well with the broken symmetry structures, but poorly with the HoD_3 structure. In simple terms the splitting into two peaks is related to the two different Wyckoff positions for the H(T) atoms in both broken symmetry structures, both of which are equally occupied by six hydrogen atoms. In the HoD_3 structure all 12 tetrahedral hydrogens correspond to a single Wyckoff position. In the broken symmetry structures all of the metal-plane H(M) hydrogens are displaced out of the metal planes. As a result of this also the H(T) atoms above the metal planes experience a different local environment than the H(T) atoms below the metal planes. These two different types of H(T) atoms thus also experience a slightly different local force fields. Although the size of the splitting of the two peaks is apparently underestimated in our calculations, the peak splitting itself can be readily understood in terms of a broken symmetry structure.

The peak around 120 meV in the experimental spectrum corresponds to bands 37–48 in Figs. 2–4 which are mainly composed of vibrations of the H(T) atoms in the ab plane, see Figs. 5 and 6. All three structures give this peak reasonably well. Only the $P6_3cm$ structure gives a feature which is clearly split with maxima at 113 and 122 meV. It is not clear to us whether or not there is a low energy shoulder below 120 meV in the experimental spectrum in Fig. 5(b). Bands 49–60 correspond to vibrations of the H(T) atoms along the c axis with energies roughly in the range 140–150 meV. Again all three structures give a density of states in this range which agrees reasonably well with experiment.

The high energy range above 150 meV is dominated by vibrations of the H(M) atoms in the ab plane corresponding to bands 61–72 in Figs. 2–4. The highest frequency peak is due to vibrations in the ab plane of the H(M) atoms that are in or closest to the metal ab plane, see Fig. 1. In the HoD_3 structure these atoms are tightly confined exactly in the metal plane in the center of an equilateral triangle of yttrium atoms, and these consequently have a high vibrational frequency of 170 meV. In the broken symmetry structures this effect is still present but weaker because these atoms are slightly out of the metal-plane. The vibrations of the H(M) atoms that are further away from the metal planes in the ab plane direction show up at a slightly lower energy around 160 meV. This peak has an intensity which is roughly twice that of the highest energy peak, which again reflects the occupancy of the corresponding hydrogen sites. In the experimental high resolution data of Ref. 29 a double peak at 157, 165 meV with the right intensity distribution can be clearly identified. The splitting agrees rather well with the broken symmetry structures and the agreement with the HoD_3 structure is slightly worse. Finally, it may be observed that the high-energy density of states above 150 meV for the $P6_3$ broken symmetry structure is in better agreement with experiment than the $P6_3cm$ broken symmetry structure, compare Figs. 5(a)–5(c). This is mainly so because the gap between the H(T) c-axis vibrations below 150 meV and the H(M) ab plane vibrations is too large in the latter structure.

Whereas the agreement between the calculated phonon density of states and the experimental NVS data is rather good for the broken symmetry structures, there are discrepancies with the density of states of the HoD_3 structure, especially in the energy range below 100 meV. Distinguishing between the two broken symmetry structures is more difficult. The calculated phonon density of states of the $P6_3$

structure gives a slightly better agreement with the experimental data in the energy range above 100 meV. This structure is also the one that has the lowest total energy in a DFT/LDA calculation.

IV. RESULTS FOR YD_3

Using the atomic force constants calculated for YH_3, it is straightforward to recalculate the phonon bands for YD_3 in the broken symmetry structure simply by doubling the corresponding masses when setting up the dynamical matrix Eq. (2). Because of the almost perfect decoupling of the hydrogen and yttrium vibrations, the low frequency yttrium modes turn out to be almost identical to those in YH_3 and the frequencies of the deuterium modes in YD_3 differ from those of hydrogen in YH_3 by almost exactly the factor $1/\sqrt{2}$ expected for simple scaling of the frequencies according to the masses. We therefore refrain from showing the YD_3 phonon bands explicitly. We next calculate the anisotropic temperature factors for the broken symmetry structure, both at zero temperature and at 295 K. The experimental data at 295 K were refined in detail by Udovic *et al.*[13] The **B** matrices of temperature factors, Eq. (5), possess the symmetry properties imposed by a particular site. **B** matrices of symmetry-related sites should transform into one another by applying the symmetry operations of the space group. These symmetry properties were checked explicitly and found to hold within 1%.

For the yttrium atoms we find almost isotropic temperature factors (which is not imposed by symmetry). The zero point motion results in an (almost) isotropic B of about 0.11 Å^2. This number increases to about 0.39 Å^2 at 300 K which is reasonably close to the experimentally determined value of 0.34 Å^2 found by Udovic *et al.* in their model II (Ref. 13) for YD_3. Direct comparison is difficult though, since the experimental data are refined assuming a different structure. For those atoms that vibrate in modes which are similar in both lattice structures, we do find values in good agreement with the experimental values. As before, we denote the deuterium atoms in the tetrahedral and metal plane positions by D(T) and D(M), respectively. For the D(T) atoms, the calculated value of B_{33} is 1.08 Å^2, the experimental value is 1.13 Å^2. The calculated numbers in the **B** matrix for the D(T) atoms which correspond to an in-plane motion are about 50 % larger.

Most interesting are the D(M) atoms, for which the thermal and zero point motion is strongly anisotropic. Because the motion of these atoms is so confined in the basal plane and so large in the c direction, the ellipsoids of vibration [Eq. (5)] for these atoms are cigar shaped. Because of the threefold rotation symmetry of this site, the **B**-matrix elements are related by $B_{11}=B_{22}=2B_{21}=2B_{12}$; consequently only the symmetry independent values B_{11} and B_{33} are given in Table IV evaluated for 295 K. At 295 K the zero point motion still accounts for more than 50% of the root mean square displacements of these deuterium atoms, so the results at zero temperature are very similar. In the broken symmetry structure the three different Wyckoff positions for the D(M) atoms are labeled with an index. $D_1(M)$ and $D_2(M)$ correspond to deuterium atoms at about 0.07 c from the metal plane, D_3(M) to atoms closer to the plane at about 0.03 c. In our calculations we have chosen a representation for the broken symmetry structure in which both $D_2(M)$ and $D_3(M)$ are *above* the metal plane.

TABLE IV. Calculated temperature factor matrix elements in Å^2 along the lattice axes for each of the Wyckoff positions of the H(M) atoms in YD_3 in the $P6_3$ structure at 295 K. These are compared to the experimental temperature factors obtained by assuming a HoD_3 structure. By symmetry, $B_{11}=B_{22}=2B_{21}=2B_{12}$. The other elements are zero by symmetry.

Atom	position	Wyckoff	B_{11}	B_{33}
		theory		
$D_1(M)$	$-0.07c$	2a	0.98	2.42
$D_2(M)$	$+0.07c$	2b	0.97	3.14
$D_3(M)$	$+0.03c$	2b	0.94	3.88
		experiment		
D($m2$)	$\pm 0.07c$	4d	0.84	2.8
D($m1$)	$0.00c$	2a	0.5	6.7

The calculated values of B_{33} are large, and largest for the $D_3(M)$ atoms which are located closest to the metal planes. The numbers extracted from experiment for out-of-plane atoms [$D(m2)$ in Ref. 13; the $D(m1)$ atoms are exactly in the metal plane] are also large. In particular, the value is huge for the deuterium atom which is assumed by Udovic *et al.* to be in the metal plane. The value of 6.7 corresponds to a root mean square displacement of about 0.3 Å which is about 1.3 % of the lattice constant in the c-direction. For hydrogen it is even larger ($\sim 0.02\ c$), and of the same order of magnitude as the size of the symmetry-breaking hydrogen displacements ($\sim 0.03\ c$) predicted from the LDA calculations.

Udovic *et al.*[25] tried to refine the diffraction data using the broken symmetry structure suggested by Kelly. Since they do not find the small additional peaks which should be present if the high symmetry is broken, they concluded that YH_3 has the HoD_3 structure. In particular, they focused on the (103) reflection, repeated the experiment at low temperature and took more data. They found no significant structure corresponding to the (103) reflection. Using the broken symmetry geometry we have calculated the Debije-Waller factors at zero temperature and compare the reduction of intensity of the (103)-reflection peak to the corresponding reduction of neighboring peaks. Although the reduction for the (103) reflection is somewhat larger than for other peaks, it is only reduced by about one third compared to the intensity in the absence of zero point motion. This is not sufficient to make this peak unobservable in the diffraction experiments. It consequently seems to rule out the possibility that the symmetry breaking is being masked in diffraction experiments by a large zero point motion. However, it does not rule out the possibility that the system is actually in a superposition of broken symmetry states. In the next section we will speculate on this possibility in more detail.

V. DISCUSSION

We have calculated the lattice vibrational properties of YH_3 and YD_3 within the harmonic approximation for three proposed lattice structures for YH_3. Apart from a calculated soft mode in the HoD_3 structure the phonon bands look quite similar for the three structures. The soft mode reflects the fact that the HoD_3 structure ($P\bar{3}c1$ symmetry) is unstable in DFT/LDA calculations.[24] The vibrational frequencies at Γ agree reasonably well with the Raman spectra of Kierey *et al.*[30] for the two broken symmetry structures which have $P6_3$ and $P6_3cm$ symmetry, respectively. On the basis of these measurements, there is no clear preference for one or the other broken symmetry structure.

The phonon bands can be divided into groups that are reasonably well separated, giving rise to distinct peaks in the phonon density of states. The latter can be compared to the experimental NVS spectrum of Udovic *et al.*[29,32] From the calculated eigenvectors we can identify for each peak in the calculated phonon density of states which atoms in which direction have a dominant contribution to the vibrations represented by that peak. The lowest frequency modes below 30 meV correspond almost exclusively to yttrium vibrations, and are comparable to the modes in pure yttrium; modes at higher energies are mainly due to motion of the hydrogen sublattice. In these modes we find distinct differences between the calculated spectra of the three suggested lattice structures. On the low energy side below 100 meV, the NVS spectrum is in poor agreement with the phonon density of states of the HoD_3 structure. The agreement with the density of states of the broken symmetry structures is clearly much better; there are only small differences between the $P6_3$ and $P6_3cm$ structures. Comparison of the data in the high energy range above 100 meV gives slightly better agreement with the $P6_3$ structure, which is also the lowest energy structure from a DFT/LDA calculation.[24]

The agreement between the NVS experimental data and the phonon density of states is not perfect. For instance, around 90 meV two peaks are found in the experiment which are split by 13 meV. The calculated splitting is only 6 and 8 meV for the $P6_3$ and $P6_3cm$ structures, respectively (and next to zero for the HoD_3 $P\bar{3}c1$ structure). This could indicate a shortcoming of the LDA in describing the energy landscape or be an indication for anharmonic effects, which we have neglected here. At this stage it is not feasible to test better approximations, but it is not urgent either since the agreement with the available experimental data is quite good. Note however that the assignments we have made for the peaks of the NVS spectrum could be checked by measurements on single crystals, which can give more detailed information.

The calculated zero point motions for the hydrogen and deuterium atoms are very large and anisotropic. This is particularly true for the H(M) atoms which are involved in the symmetry lowering when going from the HoD_3 structure to a broken symmetry structure. Since the high $P\bar{3}c1$ symmetry of the HoD_3 structure can be broken in four different but equivalent ways, the LDA Born-Oppenheimer surface has four global minima. The energy difference between the high symmetry structure and the $P6_3$ broken symmetry structure is small,[59] it is in fact smaller than the calculated total zero point energy ($\sim$60 meV) of the two modes in the $P6_3$ broken symmetry structure which are relevant for the symmetry breaking. Therefore it is not unlikely that the system is not confined in a particular $P6_3$ structure but instead in a quantum superposition of broken symmetry states. This would lead to the picture given schematically in Fig. 7. Refining the experimental powder diffraction data using all available sites in such a superposition of four representations of the broken symmetry structure is very complicated due to the large number of degrees of freedom in that case. Therefore it is not easy to prove or disprove this model by a refinement of the neutron powder diffraction data.[61] The huge temperature factors are the only experimental support at present.

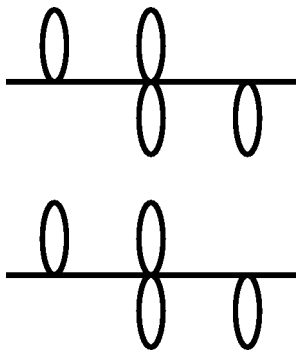

FIG. 7. Schematic picture of the quantum averaged broken symmetry structures as in Fig. 1. The ellipsoids give an impression of the quantum delocalization of the H(M) atoms.

The recent solid state NMR experiments[27] are difficult to interpret. The results of these experiments for YD_3 show that deuterium sites of different local symmetry exist in the ratio of approximately 1:1:1. In the $P\bar{3}c1$ (HoD_3) structure the ratio of hydrogen sites of different symmetry is 12:4:2, which is very different from the NMR results. For the two broken symmetry structures the 12 H(T) atoms are divided equally over two Wyckoff positions. The H(M) atoms are distributed over two Wyckoff positions in a ratio 2:1 in the $P6_3cm$ structure and equally distributed over three Wyckoff positions in the $P6_3$ structure. This would lead to a ratio of 6:6:4:2 for the $P6_3cm$ structure and 6:6:2:2:2 for the $P6_3$ structure. Thus for both these structures the splitting of the H(T) sites is compatible with the NMR results. However for the H(M) sites the NMR results indicate the presence of more symmetry than one would expect on the basis of either of the broken symmetry structures. This may point towards a quantum averaging that leads to indistinguishable NMR features for the H(M) atoms. Due to their quantum motion all of these metal plane hydrogen atoms have a large probability to be out of the metal plane, as sketched in Fig. 7. This may give rise to similar NMR patterns for all the H(M) atoms. To be consistent we have to assume, however, that the quantum motion of the H(T) atoms is smaller, since they still give rise to two different features in the NMR data.

One might wonder what the influence of the large zero point motions of the hydrogen atoms is on the band structure and, in particular, on the band gap. In a quantum averaged

picture the electronic properties are given by averaging the electronic structures corresponding to the ionic configurations encountered during the zero point motion (assuming that the Born-Opperheimer approximation does not break down and the electrons are always in their instantaneous ground state). In general, this electronic structure average can be different from the electronic structure corresponding to the average high symmetry lattice structure. However, since our recent *GW* calculations[22,23] for YH_3 result in substantial band gaps for both the HoD_3 structure and the broken symmetry structure, it is likely that the average electronic structure also has a substantial gap.

It would be very interesting to explicitly include the quantum character of the hydrogen or deuterium atoms, and to solve the Schrödinger equation for the hydrogen atoms in the potential landscape. This can be done in principle using the *ab initio* path-integral molecular dynamics method.[62] This method was recently used to include the quantum character of hydrogen in simple molecules, and clearly showed the effect of quantum tunneling of the hydrogen atoms.[63,64] Applying this method to a solid is a formidable computational task requiring at least an order of magnitude more computer time than a ''classical'' Car-Parrinello molecular dynamics simulation. Unfortunately, this is at present out of reach.

ACKNOWLEDGMENTS

We have had very useful discussions with the members of the YH_x team at Philips Research Laboratories in Eindhoven, and at the Vrije Universiteit of Amsterdam, the Netherlands. One of us (P.v.G.) also acknowledges useful discussions with G.A. de Wijs and R.A. de Groot of the University of Nijmegen, the Netherlands. This work is part of the research program of the Stichting voor Fundamenteel Onderzoek der Materie (FOM), financially supported by the Nederlandse Organisatie voor Wetenschappelijk Onderzoek (NWO) and Philips Reseach.

APPENDIX

We tested our codes by calculating phonon band structures for silicon using the direct supercell method to calculate interatomic force constants. We use a large $(5\times5\times5)$ supercell consisting of 250 silicon atoms and a smaller $(3\times3\times3)$ supercell of 54 silicon atoms. In both cases only the Γ point was used for the Brillouin zone summation. In the calculation of the phonon bands we include the force constants between the central, displaced atom, and complete shells of neighboring atoms. In the larger supercell we have neighbors up to the twelfth shell, and neighbors up to the fifth shell in the smaller supercell. Following Capaz and Joannopoulos[65] we include for both supercells one more shell of atoms in which the force constants are chosen to obey the translational sum rule exactly. In Fig. 8 we plot the phonon bands for silicon using the force constants obtained in the smaller and larger supercell, respectively. Using the larger supercell we are able to reproduce the experimental data in great detail.

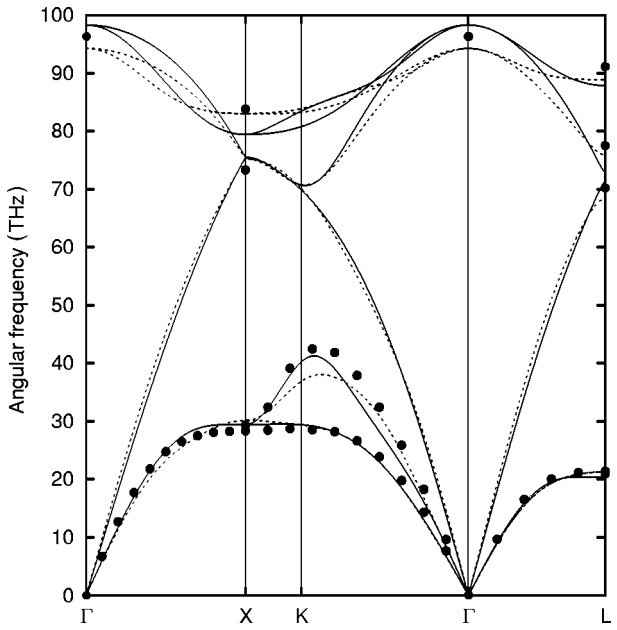

FIG. 8. Calculated phonon bands for silicon using force constants from the smaller supercell (solid lines) and the bigger supercell (dashed lines). Some experimental values taken from Ref. 67 are given by the filled circles.

The calculated frequencies at the zone boundaries agree within 3.5% with the experimental data taken from Ref. 66. Using the much smaller $(3\times3\times3)$ supercell also leads to very reasonable results. At the zone boundaries of the Brillouin zone we find discrepancies which are 6.7% or less. The ellipsoids of zero point motion are spheres for silicon as a result of full cubic symmetry. The calculated root mean square displacements are close to the experimental values,[67] both using the smaller and the larger supercell.

[1] J.N. Huiberts, R. Griessen, J.H. Rector, R.J. Wijngaarden, J.P. Dekker, D.G. de Groot, and N.J. Koeman, Nature (London) **380**, 231 (1996).

[2] F. Klose, C. Rehm, D. Nagengast, H. Maletta, and A. Weidinger, Phys. Rev. Lett. **78**, 1150 (1997).

[3] B. Hjörvarsson, J.A. Dura, P. Isberg, T. Watanabe, T.J. Udovic, G. Andersson, and C.F. Majkrzak, Phys. Rev. Lett. **79**, 901 (1997).

[4] A.T.M. van Gogh, E.S. Kooij, and R. Griessen, Phys. Rev. Lett. **83**, 4614 (1999); A.T.M. van Gogh, D.G. Nagengast, E.S. Kooij, N.J. Koeman, J.H. Rector, R. Griessen, C.F.J. Flipse, and R.J.J.G.A.M. Smeets, Phys. Rev. B **63**, 195105 (2001).

[5] M.W. Lee and W.P. Shin, J. Appl. Phys. **86**, 6798 (1999).

[6] J.H. Weaver, R. Rosei, and D.T. Peterson, Phys. Rev. B **19**, 4855 (1979).

[7] J.H. Weaver, D.T. Peterson, and R.L. Benbow, Phys. Rev. B **20**, 5301 (1979).

[8] D.J. Peterman, B.N. Harmon, J. Marchiando, and J.H. Weaver, Phys. Rev. B **19**, 4867 (1979).

[9] J.P. Dekker, J. van Ek, A. Lodder, and J.N. Huiberts, J. Phys.: Condens. Matter **5**, 4805 (1993).
[10] Y. Wang and M.Y. Chou, Phys. Rev. Lett. **71**, 1226 (1993); Phys. Rev. B **51**, 7500 (1995).
[11] M. Mannsmann and W.E. Wallace, J. Phys. (Paris) **25**, 454 (1964).
[12] N.F. Miron, V.I. Shcherbak, V.N. Bykov, and V.A. Levdik, Sov. Phys. Crystallogr. **17**, 342 (1972).
[13] T.J. Udovic, Q. Huang, and J.J. Rush, J. Phys. Chem. Solids **57**, 423 (1996).
[14] A. Remhof, G. Song, Ch. Sutter, R. Siebrecht, H. Zabel, F. Güthoff, and J. Windgasse, Phys. Rev. B **59**, 6689 (1999).
[15] A. Remhof, G. Song, K. Theis-Bröhl, and H. Zabel, Phys. Rev. B **56**, R2897 (1997).
[16] L.J. Sham and M. Schlüter, Phys. Rev. Lett. **51**, 1888 (1983); Phys. Rev. B **32**, 3883 (1985).
[17] J.P. Perdew and M. Levy, Phys. Rev. Lett. **51**, 1884 (1983).
[18] L. Hedin, Phys. Rev. A **139**, A796 (1965); L. Hedin and S. Lundqvist in *Solid State Physics*, edited by H. Ehrenreich, F. Seitz, and D. Turnbull (Academic, New York, 1969), Vol. 23, p. 1.
[19] For recent reviews of the *GW* method and its applications see F. Aryasetiawan and O. Gunnarsson, Rep. Prog. Phys. **61**, 237 (1998) or L. Hedin, J. Phys.: Condens. Matter **11**, R489 (1999).
[20] M.S. Hybertsen and S.G. Louie, Phys. Rev. Lett. **55**, 1418 (1985); Phys. Rev. B **34**, 5390 (1986).
[21] R.W. Godby, M. Schlüter, and L.J. Sham, Phys. Rev. Lett. **56**, 2415 (1986); Phys. Rev. B **37**, 10 159 (1988).
[22] P. van Gelderen, P.A. Bobbert, P.J. Kelly, and G. Brocks, Phys. Rev. Lett. **85**, 2989 (2000).
[23] P. van Gelderen, P.A. Bobbert, P.J. Kelly, G. Brocks, and R. Tolboom, Phys. Rev. B **66**, 075104 (2002).
[24] P.J. Kelly, J.P. Dekker, and R. Stumpf, Phys. Rev. Lett. **78**, 1315 (1997).
[25] T.J. Udovic, Q. Huang, and J.J. Rush, Phys. Rev. Lett. **79**, 2920 (1997).
[26] P.J. Kelly, J.P. Dekker, and R. Stumpf, Phys. Rev. Lett. **79**, 2921 (1997).
[27] J.J. Balbach, M.S. Conradi, M.M. Hoffmann, T.J. Udovic, and N.L. Adolphi, Phys. Rev. B **58**, 14 823 (1998).
[28] T.J. Udovic, Q. Huang, R.W. Erwin, B. Hjörvarsson, and R.C.C. Ward, Phys. Rev. B **61**, 12 701 (2000).
[29] T.J. Udovic, Q. Huang, and J.J. Rush, in *Hydrogen in Semiconductors and Metals*, edited by N.N. Nickel, W.B. Jackson, R.C. Bowman, and R.G. Leisure, Mater. Res. Soc. Symp. Proc. No. 513 (Materials Research Society, Pittsburgh, 1998), p. 197.
[30] H. Kierey, M. Rode, A. Jacob, A. Borgschulte, and J. Schoenes, Phys. Rev. B **63**, 134109 (2001).
[31] P. van Gelderen, P.J. Kelly, and G. Brocks, Phys. Rev. B **63**, 100301(R) (2001).
[32] T.J. Udovic, J.J. Rush, Q. Huang, and I.S. Anderson, J. Alloys Compd. **253-254**, 241 (1997).
[33] O. Madelung, *Introduction to Solid State Theory* (Springer, Berlin, 1978).
[34] P. Brüesch, *Phonons: Theory and Experiments I* (Springer, Berlin, 1982).
[35] R.M. Martin, Phys. Rev. **186**, 871 (1969).
[36] S. Baroni, P. Giannozzi, and A. Testa, Phys. Rev. Lett. **58**, 1861 (1987).
[37] P. Pavone, K. Karch, O. Schütt, W. Windl, D. Strauch, P. Giannozzi, and S. Baroni, Phys. Rev. B **48**, 3156 (1993).
[38] P. Giannozzi, S. de Gironcoli, P. Pavone, and S. Baroni, Phys. Rev. B **43**, 7231 (1991).
[39] S.Y. Savrasov, Phys. Rev. B **54**, 16 470 (1996).
[40] J. Ihm, A. Zunger, and M.L. Cohen, J. Phys. C **12**, 4409 (1979).
[41] W. Frank, C. Elsässer, and M. Fähnle, Phys. Rev. Lett. **74**, 1791 (1995).
[42] A. Eichler, K.-P. Bohnen, W. Reichardt, and J. Hafner, Phys. Rev. B **57**, 324 (1998).
[43] G. Kresse, J. Furthmüller, and J. Hafner, Europhys. Lett. **32**, 729 (1995).
[44] K. Parlinski, Z.Q. Li, and Y. Kawazoe, Phys. Rev. Lett. **78**, 4063 (1997).
[45] X. Gonze, J.-C. Charlier, D.C. Allan, and M.P. Teter, Phys. Rev. B **50**, 13 035 (1994).
[46] F. Detraux, Ph. Ghosez, and X. Gonze, Phys. Rev. Lett. **81**, 3297 (1998).
[47] K. Parlinski, Z.Q. Li, and Y. Kawazoe, Phys. Rev. Lett. **81**, 3298 (1998).
[48] X. Gonze, Phys. Rev. B **55**, 10 337 (1997).
[49] X. Gonze and Ch. Lee, Phys. Rev. B **55**, 10 355 (1997).
[50] K. Kunc and R.M. Martin, Phys. Rev. Lett. **48**, 406 (1982).
[51] G. Kern, G. Kresse, and J. Hafner, Phys. Rev. B **59**, 8551 (1999).
[52] B.T.M. Willis and A.W. Pryor, *Thermal Vibrations in Solids* (Cambridge University Press, Cambridge, 1975).
[53] G. Brocks, J. Chem. Phys. **102**, 2522 (1995); J. Phys. Chem. **100**, 17 327 (1996); Phys. Rev. B **55**, 6816 (1997); Theor. Chem. Acc. **104**, 116 (2000).
[54] R. Car and M. Parrinello, Phys. Rev. Lett. **55**, 2471 (1985).
[55] I. Stich, R. Car, M. Parrinello, and S. Baroni, Phys. Rev. B **39**, 4997 (1989).
[56] N. Troullier and J.L. Martins, Phys. Rev. B **43**, 1993 (1991).
[57] Y. Wang and M.Y. Chou, Phys. Rev. B **44**, 10 339 (1991).
[58] S.G. Louie, S. Froyen, and M.L. Cohen, Phys. Rev. B **26**, 1738 (1982).
[59] An unconstrained energy minimization invariably finds a broken symmetry structure. However, accurate determination of the energy gain requires a constrained symmetry energy minimization. The energy difference of 70 meV per Y_6H_{18} unit cell between the HoD_3 and broken symmetry structure reported in Ref. 24 was too large because in the HoD_3 calculation full relaxation of the yttrium atoms was not included. Including this relaxation lowers the energy gain to about 40 meV.
[60] S.K. Sinha, T.O. Brun, L.D. Muhlenstein, and J. Sakurai, Phys. Rev. B **1**, 2430 (1970).
[61] T.J. Udovic (private communication).
[62] D. Marx and M. Parrinello, J. Chem. Phys. **104**, 4077 (1996).
[63] D. Marx and M. Parrinello, Z. Phys. B: Condens. Matter **95**, 143 (1994).
[64] D. Marx and M. Parrinello, Science **271**, 179 (1996).
[65] R.B. Capaz and J.D. Joannopoulos, Phys. Rev. B **54**, 13 402 (1996).
[66] G. Nilsson and G. Nelin, Phys. Rev. B **6**, 3777 (1972).
[67] P.J.E. Aldred and M. Hart, Proc. R. Soc. London, Ser. A **332**, 223 (1973).